# Intensity transformation by rectangular tapered reflective coupling

M. D. Wagh and A. N. Dharamsi

A complete analysis of light propagation through a hollow coupling with a uniformly varying cross section and specularly reflecting walls is given. This enables one to relate the entrance and exit intensity distributions when the input is incoherent but collimated. Results indicate that the input aperture can be partitioned into sections characterized by the total number of reflections an incoming ray has within the coupling. Input radiation in every section is linearly spread over the entire exit aperture. Hence nonuniformities in the input intensity profile are reduced at the output. This effect can be enhanced by proper design as discussed in the paper.

## I. Introduction

Hollow structures with specularly reflecting inner walls have been used in various applications such as spatial filtering, information processing, optical communications, and energy transmission. Investigation of the transmission properties of such structures has, therefore, attracted much attention. A light pipe with a rectangular or circular uniform cross section is a relatively simple structure and has been studied by many research workers.[1–4] Conical structures with uniformly decreasing cross sections have also been examined by Williamson,[5] Loewenstein and Newell,[6] Pluchino and Moeller,[7] Hollands,[8] Wagh,[9,10] and Wijeysundera.[11] These conical structures, used as couplings between light pipes of different dimensions and as V troughs for solar energy collection, are the subject of this investigation. In particular an analysis is presented here which relates the input and output intensity distributions of a coupling with rectangular cross section (Fig. 1). The input radiation is considered to be incoherent and collimated but not necessarily aligned with the axis of the coupling. The analysis is general enough not to require any restrictions on the number of reflections that a ray makes before exiting.

The results obtained show that the number of reflections on parallel faces of the coupling by any two rays differ at the most by one. Furthermore, the entrance aperture of the coupling can be partitioned into sections, each characterized by the number of reflections on the tapering faces a ray entering within it makes before exiting. There are at the most two aperture sections corresponding to the same number of reflections. Moreover the intensity distribution in each of these sections is linearly mapped over the entire exit aperture. The total output distribution is thus obtained by summing those due to all these sections.

This characteristic of the coupling implies that any nonuniformities that may exist in the input intensity profile will be reduced at the output. A design procedure is also outlined which allows one, for example, to build a coupling (Table II, $n_1 = 4$) which can transform a displaced Gaussian intensity profile with a maximum-to-minimum intensity ratio of ~850 into an intensity profile whose maximum variation is ~4.3%. Moreover, even with as much as a 2° misalignment of the coupling, this figure changes by <2%.

## II. Statement of the Problem

In this paper a coupling of length $L$ with specularly reflecting walls and rectangular entrance and exit apertures of dimensions $2a \times 2c$ and $2b \times 2c$, respectively, is considered. It is assumed that both apertures are perpendicular to the axis of the coupling, and the entrance aperture is illuminated by a collimated incoherent beam of known intensity distribution. The geometry of the coupling, the direction of a ray, and the coordinate system used are illustrated in Fig. 1.

The aim here is to relate analytically the intensity distribution in the exit aperture with that in the entrance aperture.

The authors are with Old Dominion University, Department of Electrial Engineering, Norfolk, Virginia 23508.

Received 6 February 1981.
0003-6935/82/111922-06$01.00/0.

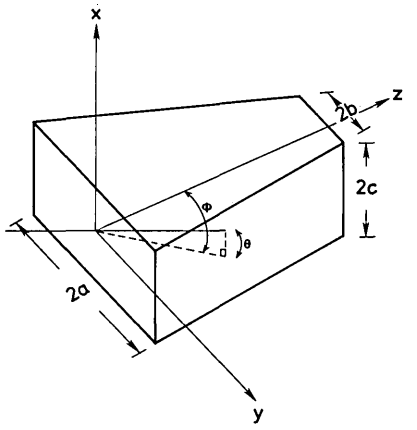


Fig. 1. Geometry of the coupling under investigation.

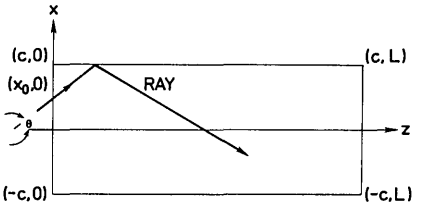


Fig. 2. Projection of the path of a ray in the coupling on an $x$-$z$ plane.

Since the input is collimated, the direction of any incoming ray is completely specified by angles $\phi$ and $\theta$. $\phi$ is the angle between the $z$ axis and the projection of the ray on the $y$-$z$ plane, and $\theta$ is the angle the ray makes with this projection. Angle $\theta$ can also be described as the angle between the $z$ axis and the projection of the ray on the $x$-$z$ plane.

The angle $\phi$, being in the $y$-$z$ plane, is unaffected by reflections on the untapered faces of the coupling as these are parallel to the $y$-$z$ plane. Similarly the angle $\theta$ is unchanged by reflections on the tapered faces since normals to these, when projected on the $x$-$z$ plane, are parallel to the $z$ axis. It is, therefore, sufficient to consider the projection of the path of a ray on the $y$-$z$ plane to compute the output $y$ coordinate, whereas a projection on the $x$-$z$ plane would yield the output $x$ coordinate.

## III. Analysis

Consider first the projection of the path of a ray on the $x$-$z$ plane as shown in Fig. 2. The only reflections which change the ray direction in this projection occur at the lines $x = \pm c$. It can be seen that in the absence of any reflections the ray entering at $x = x_0$ would emerge at $x_f = x_0 + L\tan\theta$. Each reflection on $x = \pm c$ lines decreases the exit $x$-coordinate magnitude by $2c$ and changes its sign. Consequently, the output $x$ coordinate is given by

$$x_f = (x_0 + L\tan\theta - 2kc)(-1)^k, \tag{1}$$

where integer $k$ is chosen so that $-c \leq x_f < c$ and represents the total number of reflections on the parallel faces of the coupling.

Next consider the projection on the $y$-$z$ plane shown in Fig. 3. Let a ray which has undergone $i$ reflections in the coupling make an angle $\phi_i$ with the $z$ axis. $\phi_0 = \phi > 0$ is the value of $\phi$ when the radiation enters the coupling. Now, however, unlike above, reflections occur on lines inclined to the $z$ axis, and, therefore, the analysis is somewhat more involved.

Assume for the time being that the first reflection of a ray is on the surface $S_1$. Then it follows[9] from the law of reflection that $\phi_i = (-1)^i(\phi + 2i\psi)$. Clearly

$$y_i = (-1)^{i+1}(a - z_i\tan\psi), \tag{2}$$

$$z_i = \frac{a}{\tan\psi}\left(1 - \frac{1}{T_i}\right) + \frac{z_1}{T_i}, \qquad (\psi \neq 0), \tag{3}$$

where $y_i, z_i$ are the coordinates of the $i$th reflection, and $T_i$ is defined by

$$T_i = \frac{\sin(\phi + \overline{2i-1}\psi)}{\sin(\phi + \psi)}, \qquad i = 1,2,\ldots. \tag{4}$$

We now show that the number of reflections that a ray undergoes before exiting can be determined from its entrance $y$ coordinate $y_0$. Consider a ray which emerges after $n$ reflections. For this ray,

$$z_n \leq L < z_{n+1}.$$

Using Eq. (3) to express $z_n$ and $z_{n+1}$ in terms of $z_1$ and Eq. (2) to express $z_1$ in terms of $y_1$, one gets the equivalent condition

$$T_n \leq \frac{y_1}{a - L\tan\psi} < T_{n+1}.$$

However, $y_1$ is related to $y_0$ through

$$y_1 = (y_0\tan\psi + a\tan\phi)/(\tan\psi + \tan\phi), \tag{5}$$

and $a - L\tan\psi = b$. Using these it can be shown that the entrance $y$ coordinate $y_0$ of a ray undergoing $n$ reflections in the coupling must satisfy

$$Y_n \leq y_0 < Y_{n+1}, \tag{6}$$

where

$$Y_k = \frac{bT_k(\tan\phi + \tan\psi) - a\tan\phi}{\tan\psi}, \qquad k = 1,2,\ldots. \tag{7}$$

Thus the various $Y_k$ play an important part in this analysis by defining the regions of input aperture so that

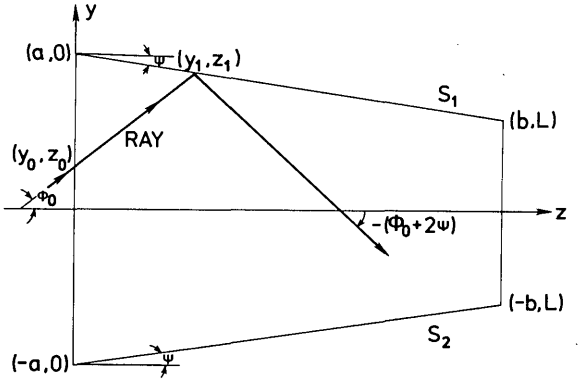


Fig. 3. Projection of the path of a ray in the coupling on an $y$-$z$ plane.

all rays with $y_0$ in the region between $Y_n$ and $Y_{n+1}$ will undergo exactly $n$ reflections in the coupling. It has already been shown[9] that the rays which undergo more than $n_{\max} = \lfloor(\pi - 2\phi)/4\psi\rfloor$ (where $\lfloor x \rfloor$ denotes the integer part of $x$) reflections in the coupling are turned back and never reach the exit aperture. Thus radiation entering the coupling between $Y_{n_{\max}+1}$ and $a$ does not contribute to the output intensity distribution. Thus to ensure that the entire input radiation with its first reflection on $S_1$ is transmitted through the coupling, $a$ should be smaller than or equal to $Y_{n_{\max}+1}$.

It may be noted that

$$T_{k+1} - T_k = 2\cos(\phi + 2k\psi)\sin(\psi)/\sin(\phi + \psi).$$

For $k \leqslant n_{\max} = [(\pi - 2\phi)/4\psi]$, $\phi + 2k\psi \leqslant \pi/2$, and, therefore, $T_{k+1} \geqslant T_k$. Using this in Eq. (7) one can see that for $k \leqslant n_{\max}$, $Y_{k+1} \geqslant Y_k$, which is consistent with inequality (6).

We now find a relation between the entrance and exit $y$ coordinates for rays originating in the region defined by (6).

Clearly the exit $y$ coordinate $y_f$ is related to the $y$ coordinate of the $n$th reflection $y_n$ by

$$y_f = y_n + (L - z_n)\tan\phi_n, \tag{8}$$

where $\phi_n$ is the angle that the ray makes after the last ($n$th) reflection. Using Eqs. (2), (3), and (5) $y_f$ can be expressed as

$$y_f = A_n + B_n y_0, \qquad y_n \leqslant y_0 < y_{n+1},$$

where

$$B_n = \frac{\tan\phi_n + (-1)^{n+1}\tan\psi}{T_n(\tan\phi + \tan\psi)},$$

$$A_n = -b\frac{\tan\phi_n}{\tan\psi} + a\frac{\tan\phi}{\tan\psi}B_n. \tag{9}$$

Now the definitions of $\phi_n$ and $T_n$ give

$$\frac{T_n}{T_{n+1} - T_n} = \frac{\tan(\phi + 2n\psi) - \tan\psi}{2\tan\psi},$$

$$\frac{T_{n+1} + T_n}{T_{n+1} - T_n} = (-1)^n\frac{\tan\phi_n}{\tan\psi}.$$

The expressions for $A_n$ and $B_n$ may, therefore, be simplified to

$$B_n = \frac{2b(-1)^n}{Y_{n+1} - Y_n},$$

$$A_n = -B_n\frac{Y_{n+1} + Y_n}{2} \tag{10}$$

to yield

$$y_f = \frac{(-1)^{n+1}b}{(Y_{n+1} - Y_n)}(Y_{n+1} + Y_n - 2y_0),$$

$$Y_n \leqslant y_0 < Y_{n+1} \tag{11}$$

This equation is of central importance as it explicitly relates the entrance and the exit coordinates of a ray traveling through the coupling. It was shown above that all the rays entering the coupling between $Y_n$ and $Y_{n+1}$ undergo exactly $n$ reflections in the coupling. Equation (11) now shows that the exit coordinates $y_f$ of these rays are linearly related to their entrance coordinates $y_0$. Moreover a ray entering at $Y_n$ exits at $(-1)^{n+1}b$, and the one entering at $Y_{n+1}$ exits at $(-1)^n b$. Thus as the entrance coordinate is varied between $Y_n$ and $Y_{n+1}$, the entire exit aperture is linearly scanned.

A similar treatment of rays whose first reflection is on $S_2$ results in a relation between the entrance and exit $y$ coordinates. This relation after some manipulation can still be expressed by Eq. (11) provided the definition of $Y_k$ is extended to nonpositive integers $k$ as

$$Y_k = \frac{bT_{-k+1}(\tan\psi - \tan\phi) + a\tan\phi}{\tan\psi}.$$

$$k = 0,-1,-2,\ldots \tag{12}$$

Note now that for the first reflection to be on $S_2$, $\phi < \psi$, and $T_k$ is a monotonically increasing function of $k$ for $0 < k < n_{\max} + 1$. Therefore, $Y_k$ defined by Eq. (12) is a monotonically increasing function for $-n_{\max} < k < 0$. This is consistent with the monotonically increasing nature of $Y_k$ when $0 < k < n_{\max} + 1$ following Eq. (7).

Thus rays entering between $Y_n$ and $Y_{n+1}$ undergo $n$ reflections on tapered faces, the first being on $S_1$, whereas rays entering between $Y_{-n}$ and $Y_{-n+1}$ also experience $n$ reflections, but the first now being on $S_2$. Rays entering between $Y_0$ and $Y_1$ exit without reflections on the tapered faces.

The condition for all the input radiation with the first reflection on $S_2$ to be transmitted is $Y_{-n_{\max}} < -a$, which reduces to $a < bT_{n_{\max}+1}$ (if it is recalled that $\phi < \psi$ in this case). Similarly the condition for all the input radiation with first reflection on $S_1$ to be transmitted is $a < Y_{n_{\max}+1}$, which also reduces to $a < bT_{n_{\max}+1}$. Thus the only design criterion that needs to be satisfied to ensure that all the input radiation is transmitted is $a < bT_{n_{\max}+1}$. This is consistent with (14) of Ref. 9.

## IV. Discussion and Conclusions

Results of the analysis of Sec. III can be summarized as follows:

(1) The entrance and exit $x$ coordinates of any ray propagating through the coupling are in one–one linear correspondence with each other. Furthermore, the exit $x$ coordinate depends solely upon the entrance x coordinate, length $L$ of the coupling, and inclination $\theta$ of the ray [Eq. (1)].

(2) Along the $y$ direction, the entrance aperture can be partitioned into sections so that all the rays starting in the same section undergo an equal number of reflections on the tapered faces of the coupling [Eqs. (6) and (7)].

(3) The $y$ coordinates of the rays entering any of these input aperture sections are in one–one linear correspondence with the $y$ coordinates of the entire exit aperture. Furthermore, this correspondence depends only upon the entrance $y$ coordinate, the input aperture section to which it belongs, length $L$, and angle $\psi$ of the coupling and inclination $\phi$ of the ray [Eq. (11)].

Using the above results calculation of the intensity distribution at the exit aperture is relatively simple. Since every input aperture section is being linearly projected on the complete exit aperture, the intensity

at the output due to a section between, say, $Y_n$ and $Y_{n+1}$ is attenuated by the factor $2b/(Y_{n+1} - Y_n)$. Furthermore, the assumption of incoherence allows the total output distribution to be obtained by a summation of all such distributions due to different sections. The intensities in the output and input planes $I_f$ and $I_0$, respectively, can now be related as

$$I_f(x_f,y_f) = \sum_{n=-n_{\max}}^{n_{\max}} \frac{(Y_{n+1} - Y_n)}{2b} I_0(x_0,y_0), \qquad (13)$$

where $x_0$ is obtained from $x_f$ using Eq. (1), $y_0$ is computed for each $n$ from $y_f$ using Eq. (11), and $I_0$ is assumed to be zero outside the entrance aperture.

An immediate consequence of the fact that the flux from each input aperture section is distributed linearly over the entire exit aperture is that any nonuniformities in the input distribution are reduced at the output. This is further brought out by the following relation between $(dI_f^n/dy_f)$ and $(dI_0/dy_0)$.

Let $Y_n \leqslant y_0 < Y_{n+1}$ and $I_f^n$ denote the intensity at the exit aperture due to the rays entering between $Y_n$ and $Y_{n+1}$. Obviously

$$I_f = \sum_{n=-n_{\max}}^{n_{\max}} I_f^n .$$

Then from Eq. (11)

$$dy_f = \frac{(-1)^n 2b}{Y_{n+1} - Y_n} \cdot dy_0, \qquad Y_n \leqslant y_0 < Y_{n+1}. \qquad (14)$$

Also, from the energy conservation principle, which led to Eq. (13),

$$dI_f^n(x_f,y_f) = \frac{Y_{n+1} - Y_n}{2b} dI_0(x_0,y_0) \qquad Y_n \leqslant y_0 < Y_{n+1} \qquad (15)$$

From Eqs. (14) and (15),

$$\frac{dI_f^n(x_f,y_f)}{dy_f} = \left(\frac{Y_{n+1} - Y_n}{2b}\right)^2 (-1)^n \frac{dI_0(x_0,y_0)}{dy_0} . \qquad Y_n \leqslant y_0 < Y_{n+1} \qquad (16)$$

Equation (16) shows that decreasing input aperture section $Y_{n+1} - Y_n$ reduces the output nonuniformities (rate of output intensity variation w.r.t. $y$ coordinate) in a quadratic manner. From Eqs. (7) and (12)

$$\frac{Y_{n+1} - Y_n}{2b} = \frac{\cos(\phi + 2|n|\psi)}{\cos\phi} R, \qquad (17)$$

where $R = 1$ for $n \geqslant 0$ and $R = \sin(\psi - \phi)/\sin(\phi + \psi)$ for $n < 0$.

Therefore, the input intensity nonlinearities in sections corresponding to larger number of reflections $|n|$ are suppressed much more effectively than those for smaller $|n|$.

Another important design criterion is the finite extent of input aperture which introduces discontinuities in $I_0$ by forcing $I_0(y_0) = 0$ whenever $y_0 > a$ or $y_0 < -a$. So that these discontinuities are not transferred to the exit aperture, one should ensure that points $\pm a$ coincide exactly with $Y_{n_1}$ and $Y_{n_2}$, respectively.

When $\phi < \psi$, $n_2$ is negative. In this case the equalities can be simultaneously satisfied by choosing the coupling parameters so that

$$\frac{a}{b} = T_{n_1} = T_{-n_2+1}. \qquad (18)$$

This is easily verified from Eqs. (7) and (12). Equation (18) also shows that in this case $n_2 = -n_1 + 1$. Thus there are as many input aperture sections with first reflection on $S_2$ as there are with first reflection on $S_1$. Obviously, since $T_{n_1}$ depends on $\phi$ a coupling designed for a particular $\phi$ using Eq. (18) will not perform optimally if the input radiation orientation $\phi$ is changed. Tables I and II show the effect on the output unifor-

**Table I. Dependence of the Uniformity of Output Intensity Profile on the Coupling Design ($a/b$ Ratio) and the Alignment Error ($\phi$) when the Input Profile is Gaussian (max/min Intensity Ratio at the Input = 20.079) and $\psi = 6°$**

| $n_1$ | Max no. of reflections for $\phi = 0$ | $a/b$ Ratio | Max/min intensity ratio at the output | | | | |
|---|---|---|---|---|---|---|---|
| | | | $\phi = 0°$ | $\phi = 0.5°$ | $\phi = 1.0°$ | $\phi = 1.5°$ | $\phi = 2.0°$ |
| 2 | 1 | 2.956 | 1.040 | 1.301 | 1.626 | 1.952 | 2.225 |
| 3 | 2 | 4.783 | 1.019 | 1.077 | 1.331 | 1.169 | 1.189 |
| 4 | 3 | 6.401 | 1.014 | 1.029 | 1.056 | 1.064 | 1.074 |
| 5 | 4 | 7.740 | 1.012 | 1.026 | 1.031 | — | — |
| 6 | 5 | 8.740 | 1.011 | 1.017 | — | — | — |
| 7 | 6 | 9.358 | 1.010 | — | — | — | — |
| 8 | 7 | 9.567 | 1.010 | — | — | — | — |

**Table II. Dependence of the Uniformity of Output Intensity Profile on the Coupling Design ($a/b$ Ratio) and the Alignment Error $\phi$ when the Input Profile is Displaced Gaussian (max/min Intensity Ratio at the Input = 853.461) and $\psi = 6°$**

| $n_1$ | Max no. of reflections for $\phi = 0$ | $a/b$ Ratio | Max/min intensity ratio at the output | | | | |
|---|---|---|---|---|---|---|---|
| | | | $\phi = 0$ | $\phi = 0.5°$ | $\phi = 1.0°$ | $\phi = 1.5°$ | $\phi = 2.0°$ |
| 2 | 1 | 2.956 | 2.615 | 2.101 | 1.759 | 1.482 | 1.276 |
| 3 | 2 | 4.783 | 1.122 | 1.163 | 1.207 | 1.201 | 1.157 |
| 4 | 3 | 6.401 | 1.043 | 1.093 | 1.079 | 1.077 | 1.061 |
| 5 | 4 | 7.740 | 1.021 | 1.074 | 1.028 | — | — |
| 6 | 5 | 8.740 | 1.010 | 1.022 | — | — | — |
| 7 | 6 | 9.358 | 1.006 | — | — | — | — |
| 8 | 7 | 9.567 | 1.005 | — | — | — | — |

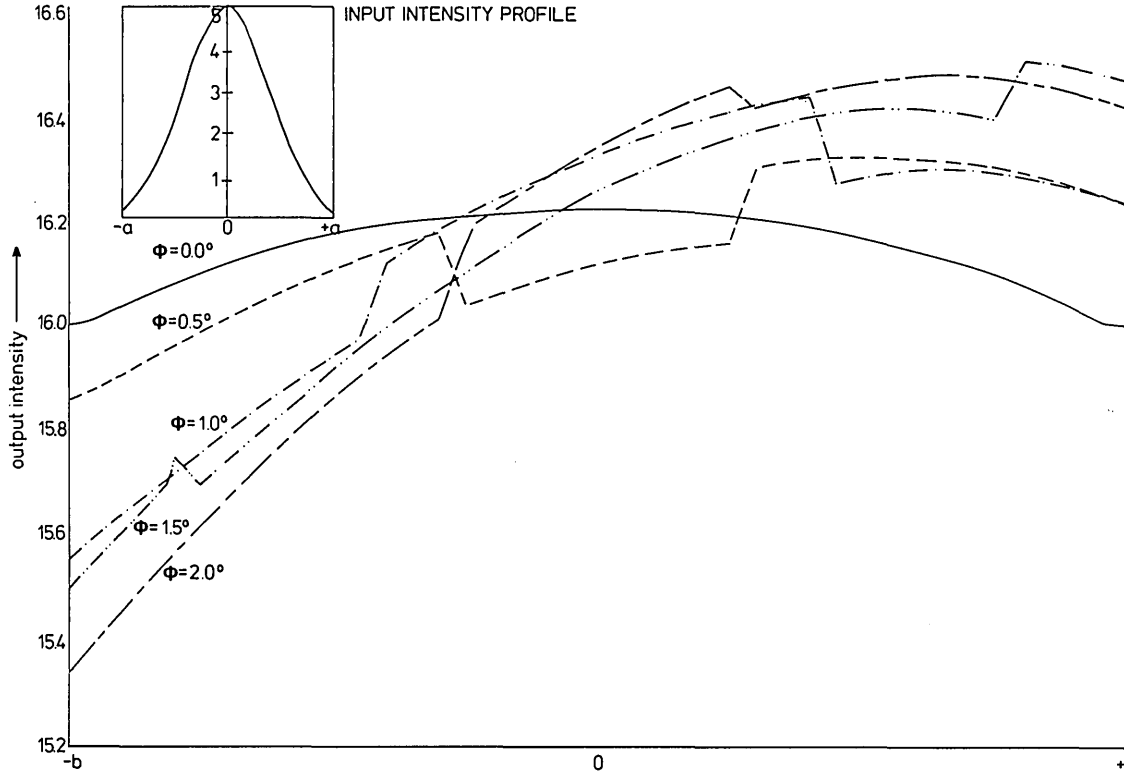


Fig. 4. Transformation of a Gaussian intensity profile by a coupling designed for input radiation angle of 0, $a/b = 6.4$, and $\psi = 6°$. (The intensity scales in the figure have arbitrary units.)

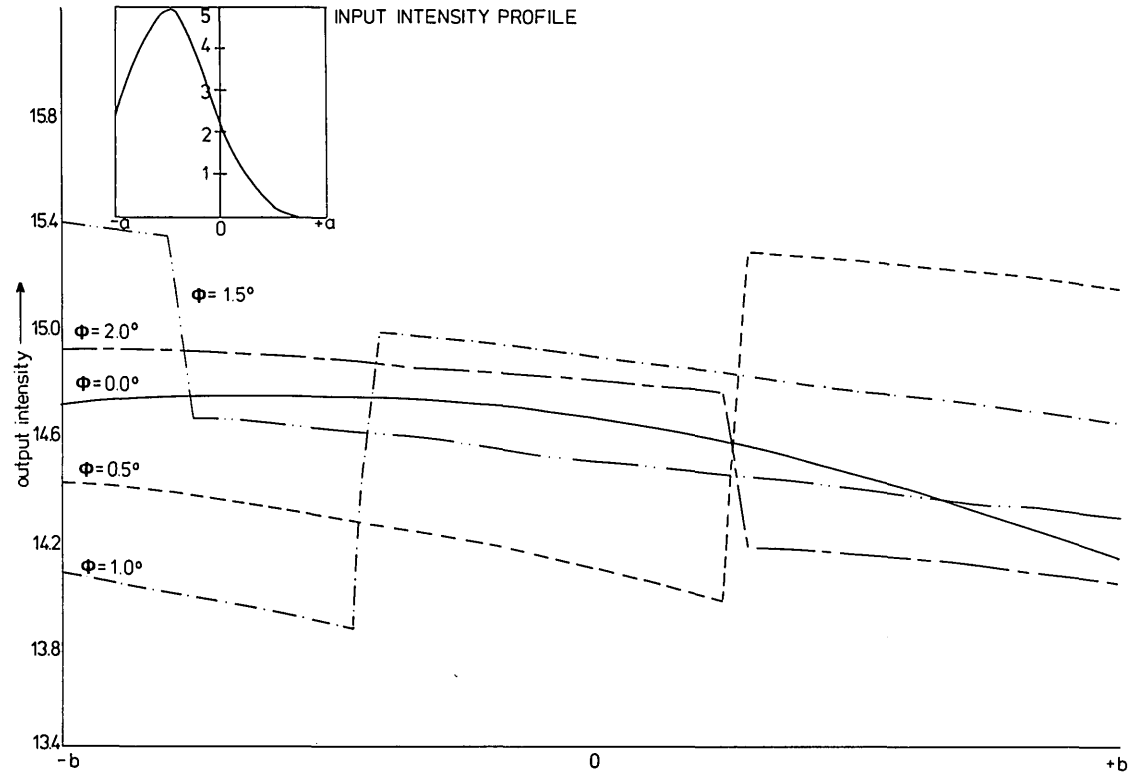


Fig. 5. Transformation of a shifted Gaussian intensity profile by a coupling designed for the input radiation angle of 0, $a/b = 6.4$, and $\psi = 6°$. (The intensity scales in the figure have arbitrary units.)

mities of an error in the orientation angle $\phi$. All seven couplings are designed from Eq. (18) using $\phi = 0$. The entrance intensity profile used for calculating results in Tables I and II are shown in the insets in Figs. 4 and 5, respectively. As expected, for both cases the nonuniformity at the output (as measured by the maximum-to-minimum intensity ratio) increases as alignment error in a particular coupling increases. Also as expected from Eq. (17), the nonuniformity at the output can be decreased by using a coupling with a larger $n_1$. Such a coupling is also relatively insensitive to alignment errors as can be observed by comparing the performances of couplings with $n_1 = 2$ and 4 in Tables I and II. The price of this better performance is the increased $a/b$ ratio or equivalently an increased length $L$. Note that the blanks in these tables correspond to cases for which all the input radiation is not transferred to the output as discussed at the end of Sec. III.

Figures 4 and 5 show the transformation of intensity profiles by a coupling designed using Eq. (18) with $n_1 = 4$, $\psi = 6°$, and $\phi = 0$. It can be seen that when the input radiation orientation $\phi$ matches the design value ($\phi = 0$), the output profile is smooth. However, a mismatch between the design and actual values of $\phi$ results in discontinuities in output profile. This, as discussed above, is due to the mismatch between the $Y_n$ values and discontinuities in the input profile at $\pm a$ forced by the finite input aperture. Consequently in general each curve with mismatched $\phi$ has two discontinuities as is borne out by Fig. 4. The input profile of Fig. 5, however, has only one large discontinuity at $-a$, and, therefore, the resultant output profiles (for $\phi = 0$) have a single large discontinuity each.

In spite of the discontinuities discussed above, Tables I and II and Figs. 4 and 5 show that the couplings are able to smooth out to a large extent any discontinuities present in the input intensity profiles even when there are small mismatches between the design and experimental conditions. This immediately suggests that such couplings can be used in applications requiring uniform distributions of the input energy over a given target.

The analysis given here has assumed that the reflectivity of the coupling walls $\rho$ is unity. In the event that this is not so, one can still use the results obtained by modifying them appropriately. From Eq. (1) it is easy to see that the number of reflections on the parallel faces of the coupling equal

$$\left\lfloor \frac{x_0 + L\tan\theta}{2c} + \frac{1}{2} \right\rfloor .$$

Thus when $x_0$ goes from $-c$ to $+c$, the number of reflections on parallel faces change at most by one. Denoting $[(L\tan\theta)/2c]$ by $m$, we find that the number of reflections on parallel faces $n'$ equal $m$ if

$$-c \leqslant x_0 < 2cm - L\tan\theta + c,$$

and $m + 1$ if

$$2cm - L\tan\theta + c \leqslant x_0 \leqslant c. \tag{19}$$

Finally the relation (13) between the entrance and exit intensity distributions will now have to be modified to

$$I_f(x_f, y_f) = \sum_{n=-n_{\max}}^{n_{\max}} \left( \frac{Y_{n+1} - Y_n}{2b} \right) \rho^{|n| + n'} I_{0(x_0, y_0)}. \tag{20}$$

In conclusion it might be pointed out that the only assumptions used in this analysis are those of incoherence and collimation of the input beam making this analysis widely applicable. Its generality can be illustrated, for example, by noting that some of the results in Refs. 8 and 11 could be obtained from results by choosing a coupling so that $a = Y_2$.

## References


1. P. G. Frame, Br. J. Appl. Phys. **1**, 741 (1968).
2. T. O. Poehler and R. Turner, Appl. Opt. **9**, 971 (1970).
3. W. R. Powell, Appl. Opt. **13**, 952 (1974).
4. E. Garmire, T. R. McMahon, and M. Bass, Appl. Opt **15**, 145, 2028 (1976).
5. D. E. Williamson, J. Opt. Soc. Am. **42**, 712 (1952).
6. E. V. Loewenstein and D. C. Newell, J. Opt. Soc. Am. **59**, 407 (1969).
7. A. Pluchino and K. D. Moeller, Appl. Opt. **10**, 1694 (1971).
8. K. G. T. Hollands, Sol. Energy **13**, 149 (1971).
9. M. D. Wagh, Appl. Opt. **15**, 2840 (1976).
10. M. D. Wagh, Appl. Opt. **15**, 2844 (1976).
11. N. E. Wijeysundera, Sol. Energy **19**, 583 (1977).